PHYSICAL REVIEW E **71**, 010902(R) (2005)

Inertia of amoebic cell locomotion as an emergent collective property of the cellular dynamics

Shin I. Nishimura[1] and Masaki Sasai[1,2]
[1]*Department of Complex Systems Science, Graduate School of Information Science, Nagoya University, Nagoya 464-8601, Japan*
[2]*Institute for Advanced Research, Nagoya University, Nagoya 464-8601, Japan*
(Received 4 June 2004; published 14 January 2005)

Amoebic cells are ubiquitous in many species and have been used as model systems to study the eukaryotic cellular locomotion. We construct a model of amoebic cells on two-dimensional grids, which describes sensing, cell status, and locomotion in a unified way. We show that the averaged position of simulated cells is described by a second-order differential equation of motion and that the mechanical pushing at the initial moment boosts the cell movement, which continues after the cell is released from the pushing. These "inertialike" features suggest the possibility of Newtonian-type motions in chemical distributions of the signaling molecule. We show, as an example, the possibility of rotating motion in a "centripetal" distribution. The observed inertial motion is an emergent collective dynamics, which is controlled by diffusive and chemical processes in the cell.

DOI: 10.1103/PhysRevE.71.010902 PACS number(s): 87.17.Jj, 87.16.Qp, 87.16.Xa, 87.17.Aa

How does a cell sense the distribution of signaling molecules in environment and move in response to it? The motional response of eukaryotic cells has been extensively studied by using amoebic cells as model systems [1]. Amoebic cells can move toward the gradient of concentration of chemoattractants such as cyclic adenosine mono phosphate (cAMP) for a slime mold, *Dictyostelium dicoideum* [2], or formyl leucin methionin phenylalanine (fMLP) for neutrophils [3,4]. Such behavioral response of cells is called chemotaxis. In chemotaxis an amoebic cell detects the difference in concentration of chemoattractant between the rear and front of the cell [5], and the mechanism to detect such a small difference in the noisy environment has been an important subject to be studied [6]. Amoebic cells, however, do not always follow the gradient but also show a variety of different behaviors. For example, Jeon *et al.* [7] constructed the one-dimensional "hill" gradient in which the concentration initially increases but decreases from a "top" position. They observed that cells starting from a bottom edge of the gradient passed the top and went against the gradient for a moment until they returned. Neutrophils and other amoebic cells can spontaneously move in nondefinite directions under the uniform increase in the concentration of chemicals, showing the behavior called "chemokinesis" [4]. Even without chemoattractants, cells continue to move in one direction when they are mechanically pushed forward at the initial moment [8]. These rich behaviors suggest that there is no one-to-one correspondence between the environment and the behavior, but that the cell movement depends on both the environment and the cell status simultaneously, leading to the nonlinear and history-dependent response to the environment. The purpose of this Rapid Communication is to explain the rich behaviors of cells by taking into account the sensing, cell status, and locomotion in a unified model. We propose a perspective that the cell motion is described as a collective dynamics emerging from the system of many degrees of freedom, which should offer language and techniques to study cell behaviors.

Both sensing and locomotion mechanisms of amoebic cells have begun to be elucidated at the molecular level [9]. Cellular locomotion is promoted by the dynamical change of concentration of actin filaments in the cell, i.e., by the balance between the binding and removing of actin monomers to and from the filament. We describe these molecular features with a simplified model defined on two-dimensional hexagonal grids. Two-dimensional grids have also been used to study the cellular motion in models of morphogenesis [10,11].

A grid within the cell domain is called "cellular grid," and a grid out of the cell is an "environmental grid." If a cellular grid has less than six nearest cellular grids, or equivalently, if it has at least one neighboring environmental grid, we call it a "membrane grid." At each grid, the local concentration of molecules, S_j, A_j, I_j, and F_j are defined. Here, the concentration of the chemoattractant, S_j, is nonzero only at the environmental or membrane grids, whereas concentrations of activator and inhibitor, A_j and I_j, and the concentration of actins in a polymerized filamentary form, F_j, are nonzero only at cellular grids. Changes in those concentrations and in the cellular shape are simulated with a Monte Carlo–type stochastic algorithm. We define several events in the simulation: (1) chemical kinetics, (2) diffusion, (3) cellular extension, (4) cellular shape maintenance, and (5) sampling.

The definition of the event of chemical kinetics is based on the model of Levchenko *et al.* [5]. At first, the event randomly selects a cellular grid. Here, we may use the suffix j to specify the selected grid. A_j, I_j, and F_j are updated to A_j', I_j', and F_j' by the following rules:

$$A_j' = A_j + \alpha S_j - k_\alpha A_j, \tag{1}$$

$$I_j' = I_j + \beta S_j - k_\beta I_j, \tag{2}$$

$$F_j' = F_j + \begin{cases} \gamma - k_f F_j & \left(\dfrac{A_j}{I_j} > h\right) \\ -k_f F_j & (\text{otherwise}), \end{cases} \tag{3}$$

where α and β are rates of increase in the activator and inhibitor induced by the chemoattractant reception at the membrane, and γ is the rate of actin polymerization promoted when the ratio of activator to inhibitor exceeds a

threshold, h, k_α, k_β, and k_f are rates of degradation.

We assume that only the inhibitor can diffuse across cellular grids. The event of diffusion randomly selects a cellular grid. If the selected grid and its nearest cellular grids are denoted by j and l, respectively, inhibitor molecules are redistributed by the following rules: $I_j' = I_j - DI_j$, $I_l' = I_l + DI_j/n$, where D is a constant and n is the number of the nearest cellular grids to j. D is smaller than one by definition.

When actin filaments accumulate to exceed a certain threshold, the cellular domain extends outward. The event of "cellular extension" randomly selects a membrane grid. If F_j is larger than a threshold $F_{\rm th}$ at the selected grid j, the rule generates a new cellular grid (referred to as k) by changing the environmental grid adjacent to the jth grid into a cellular grid. If two or more adjacent grids are environmental, then one of them is randomly selected to be cellular. Actin filaments are equally divided into grids j and k as $F_j' = F_j/2$ and $F_k' = F_j/2$.

The surface tension should suppress the cellular extension. Here, we use the term "volume" as the number of cellular grids. The surface tension is modeled by the tendency for the cellular volume to have an equilibrium value and by the tendency for the cellular membrane to be as small as possible. The event of cellular shape maintenance selects a membrane grid and decides whether the grid is removed from the cell to become environmental or a new cellular grid is added at the adjacent position to the selected one by estimating a cost function, $E = (V - V_0)^2 + cL^2$, where V and L are the cellular volume and length of the membrane, respectively, and V_0 and c are constants. Because the cellular surface is elastically maintained with various skeleton structures, we adopted the form of E having a term proportional to L^2 instead of L. If E' denotes the cost function after either a cellular grid is removed or added, we "undo" the event of removing and/or adding with the probability, $P_e = \max[1 - e^{(E'-E/T)}, 0]$. If the event of removing is selected, local concentrations of A, I, and F in the grid are added into one of its nearest cellular grids, which is randomly selected if there are two or more nearest grids. Note that if the cell is disconnected into multiple domains by removing a grid, the removing is canceled and another grid is selected. This procedure prevents the cell from breaking into pieces.

The event of sampling does not alter the system but the cellular shape, position, and concentrations of molecules are monitored. "One step" of the cellular dynamics is counted when sampling is called once.

We also give a "master" rule that randomly selects one of the above five events to be executed. The probabilities to select one of those five events are P_i with $i = 1$–5 and $\Sigma_{i=1}^{5} P_i = 1$. The master rule is called several million times in one trajectory of the cellular locomotion.

We assume that the length of a grid is approximately 1.0 μm. Correspondingly to the typical size of a neutrophil, several 10 μm, we put the initial shape of the cell to be a circle with a 30-grid diameter, and the equilibrium volume is set to be $V_0 = 900$. We assume that the event of diffusion is more frequent than the other chemical or cellular events as $P_2 \gg P_1 \approx P_3 \approx P_4 \gg P_5$. The effective diffusion constant of the inhibitor is $D_{\rm eff} \equiv (D/6)(1.0\ \mu{\rm m})^2/\delta t \times (P_2/P_5)/V_0$,

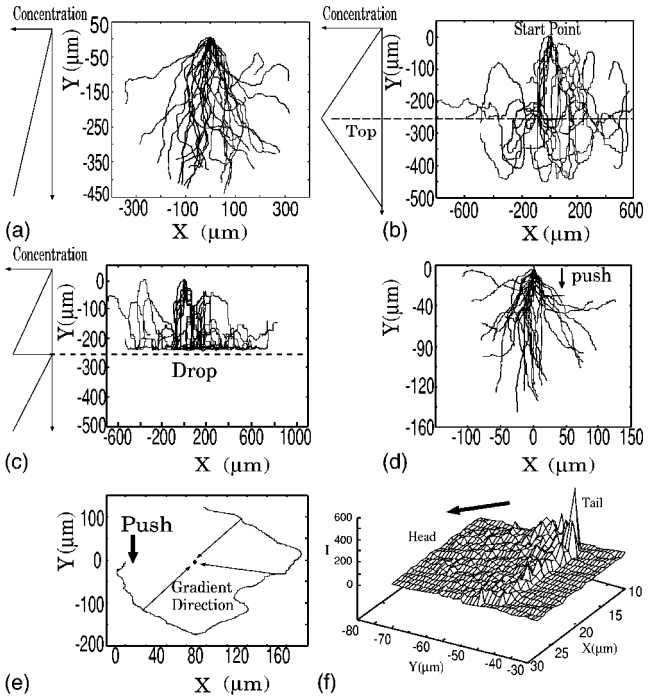

FIG. 1. (a)–(e) Trajectories of cells. The trajectories in each figure are the positions of cells obtained by repeated independent simulations with the same initial conditions, and with the same parameters but with different random number realization. (a) The trajectories in a linear gradient. The direction of the gradient is downward (20 031 steps in total). (b) A hill gradient. A dashed line indicates the top of the gradient. The ascent slope to the top has the same gradient as the linear gradient in a (13 791 steps). (c) A cliff gradient. The concentration increases downward but suddenly drops at a line (13 796 steps). (d) The uniform concentration, $S = 1$. Cells are pushed at the initial position. (Initial pushing: 1000 steps, 1780 steps in total). (e) A trajectory in a "centripetal" gradient. The cell starts from the point (0,0) and the center is at (70,0). The cell is pushed downward during a short period of starting steps. (Initial pushing: 1000 steps, 9170 steps in total). (f) The distribution of the inhibitor in a cell (1199th step in the linear gradient). The cell spreads on the xy plane. The vertical axis indicates the local concentration of the inhibitor.

where δt is the time length of one step. By setting $\delta t = 0.3$ s, $P_2 = 0.899$, $P_5 = 0.0003$, and $D = 0.45$, we have $D_{\rm eff} \approx 0.8\ \mu{\rm m}^2/{\rm s}$, which is of the same order of the diffusion constant of proteins in a bacterium. Other parameters are set to prevent the actin filament from spreading too broadly along the membrane but to be heterogeneously distributed in response to the anisotropic environmental stimuli [2]: $\alpha = 1.0$, $\beta = 0.1$, $k_\alpha = 0.9$, $k_\beta = 0.02$, $\gamma = 4.0$, $k_f = 0.99$, $h = 10.0$, $F_{th} = 1.0$, $P_1 = 0.0419$, $P_3 = 0.0299$, $P_4 = 0.0299$, $c = 1.2$, and $T = 100$.

First, we investigate the cell behavior in the two-dimensional xy plane under the linear gradient, $S_j = ay + b$, with $a = -1$ and $b = 30$. Figure 1(a) shows trajectories in this linear gradient, each of which is generated by using a different random number seed. All the trajectories are simulated with the same set of parameters and started from the same initial point, (0,0). Although the chemical gradient here is as small as $|\partial S/\partial y|/S \sim 0.01$–$0.001/\mu$m, cells go toward the

gradient as was observed in [2]. They show a large diffusive fluctuation along the x direction. The averaged chemotactic velocity along the y direction is about 0.03 grid/step, which roughly coincides with the observed speed of a neutrophil, 0.1 μm/s [4].

We next investigate cellular behaviors in more complex gradients: hill and cliff gradients. In the hill gradient, the cell moves beyond the top position until it returns [Fig. 1(b)], while in the cliff gradient, the cell cannot go beyond the drop as if there exits a repulsive wall [Fig. 1(c)], showing the same behaviors as were observed by Jeon *et al.* [7]. In our simulations the scale of spatial variance, 250 μm from bottom to top or to the drop, is almost identical to that in the experimental setup in [7]. Cells proceeded $(1.29\pm0.58)\times10^2$ μm beyond the top of the hill in our simulation, which roughly reproduces the experimental result on the distance that cells moved beyond the top, $(0.8\pm0.4)\times10^2$ μm. Here, the latter was estimated from six cellular trajectories shown in [7].

The cell shows behavioral responses not only to the chemical gradient but also to the mechanical stimuli. Fig. 1(d) shows trajectories in a uniform chemical concentration, $S=1$. Cells are pushed initially in the simulation by introducing an additional "pushing" event defined as follows: first a membrane grid j is randomly selected. If the vertical position y of the jth grid is larger than the threshold y_0, then the grid is removed. Local concentrations of A_j, I_j, and F_j in the grid are added into one of its nearest cellular grids randomly selected. This event has an effect as if to push the cell by a plank. y_0 is set to 7.5, about a half of the cellular radius. This pushing event is selected by the master rule with the probability $P_6=0.23$ and other events are suppressed with the decreased probabilities of $P_i(1–P_6)$ for $i=1–5$. After the 1000th step, P_6 is set to 0 and the cell is released to move without being forced. Even after releasing, the cell proceeds with keeping its initial motional direction, reproducing the experimental observation in [8].

The above results in the hill gradient or with the pushing at the initial phase imply that cells behave as if they had "inertia" of motion. If this is the case, we may expect that cells exhibit various Newtonian type motions. The cell in a centripetal gradient, for example, should rotate around the center if its initial velocity has a component vertical to the radial direction, i.e., nonzero "angular momentum." We assume a fixed density distribution of chemoattractant as $S_j=S_0-d|\vec{r}_j-\vec{r}_0|^2$, where $\vec{r}_j$ is a position, $\vec{r}_0$ is a center, and d and S_0 are constants. We use $d=1.0$ and $S_0=4\times10^4$. Indeed, the cell in this gradient does not direct to the center immediately but keeps rotating for a certain angle width. There is a large fluctuation in this persistent angle of rotation depending on the random number seed used in the simulation. As exemplified in Fig. 1(e), we can often find trajectories that rotate for more than π.

This inertia is a collective property emerging from the originally overdamped dynamics. In the cellular locomotion the cell extracts the rear and extends the front at the same time, which increases the inhibitor density at the rear and decreases it at the front. Thus generated inhomogeneity in the inhibitor distribution further promotes the forwarding movement of the cell and stabilizes the distribution of the inhibitor self-consistently. An example of the self-consistent inhibitor distribution is shown in Fig. 1(f). In this example, the gradient $|\partial I/\partial y|/I\sim0.1/\mu$m is much larger than $|\partial S/\partial y|/S\sim0.01$–$0.001/\mu$m. Note that since the activator does not diffuse, it is distributed into a narrow area around the membrane. The cell tends to keep moving as if it had inertia as far as such a pattern of the inhibitor is kept, so that the mass of the inertial motion should be correlated to the lifetime of the inhibitor distribution pattern. We may expect that the faster the inhibitor diffuses, the shorter the lifetime of the pattern is. Because D_{eff} is proportional to P_2, the larger P_2 should yield the smaller inertial effect in the model. The anticorrelation between P_2 and inertia is verified in the results shown in Fig. 2, where cells move in the hill gradient whose top is at $y=-80$. For each value of P_2, ten trajectories were simulated with the starting point at $y=0$ and the farthest reaching position at which the trajectory reversed its direction was monitored. The point is plotted at various P_2, suggesting that the mass decreases as P_2 increases.

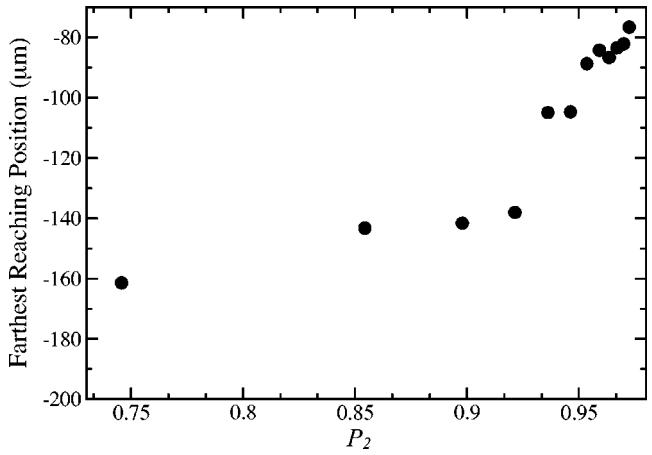

FIG. 2. The farthest reaching position of ten trials of cellular locomotion in a hill gradient is plotted for each value of P_2, the probability of the diffusion event to be selected. As P_2 becomes large, D_{eff} increases and P_i with $i\neq2$ decreases. Trajectories start from $y=0$. The top of the gradient is at $y=-80$. When P_2 is large, the farthest reaching position comes close to -80, showing the loss of ability to go beyond the top.

More quantitative analysis is possible by comparing the simulated data with the equation of motion,

$$m\frac{d^2\vec{r}}{dt^2}=\nabla S/S-k\frac{d\vec{r}}{dt}, \tag{4}$$

where $\vec{r}$ is the center position of cell, S indicates the field of concentration of chemoattractant, and m and k are effective mass and damping rate. We emphasize that the effective mass here is completely different form the real mass but it represents a memory effect in the cellular motion. These mass and damping rates should be determined by the parameters of intracellular molecular processes. By substituting $S=ay+b$ with $a=1$ and $b=30$, solutions of Eq. (4) roughly fit the time evolution of the averaged position of ensemble of simulated cells in the linear gradient. Figure 3 shows that the averaged positions of cells are well fitted by solutions of Eq.

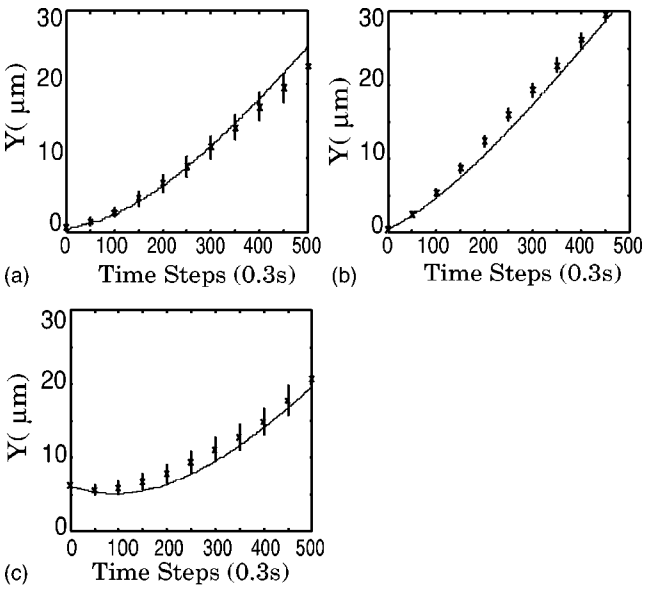

FIG. 3. Solutions of the equation of motion are compared with the simulated data. The crosses and bars indicate the averaged position of cells and their error bars are estimated from the standard deviation, respectively. In each figure the average was taken over ten independent trajectories starting from the same initial condition but with different random number seeds. Solid curves indicate solutions of equation $125\ddot{y}=1/(y+30)-0.25\dot{y}$. (a) The averaged initial velocity is small. (b) Cells are initially pushed forward to make the averaged initial velocity positive. (c) Cells are initially pushed backward to make the averaged initial velocity negative.

(4) at least during the short-time interval. Three subfigures correspond to three different initial positions and velocities and are fitted by using the same parameter values $m=125$ and $k=0.25$ in Eq. (4). Notice that force in Eq. (4) is $\nabla S/S$ instead of ∇S. Better fitting of $\nabla S/S$ than ∇S to the simulated results is consistent with the experimental observation that the chemotaxis is not driven by the absolute amplitude in concentration of chemicals but by its gradient: the uniform increase of the concentration gives rise to "adaptation," the inert response of cells [2].

In this Rapid Communication we introduced a model of amoebic cells, which describes sensing, cell status, and locomotion in a unified way. The simulated cellular trajectories in the hill gradient or those after the mechanical pushing showed that the cell locomotion has inertialike characteristics. The averaged motion in the linear gradient is described by a second-order differential equation of motion. These observations, à la Galileo, suggest that Newtonian-type motions are possible. Indeed, the rotational motion is possible in the simulation in the centripetal chemical distribution, and its experimental verification should be an interesting subject to be pursued.

It would be also interesting to analyze not only the averaged behavior of the ensemble of cells but also fluctuations in the individual cells. Each cell shows the diffusive fluctuating motion around the average course described by Eq. (4) of motion. Statistics of these fluctuations is yet to be elucidated, raising questions on the statistical mechanics of cellular movements. Another statistical physical question is how the effective mass and the damping rate in the equation of motion are explained from chemical and diffusive parameters of intracellular molecular processes. In the present work mass was shown to be anticorrelated to the diffusion constant of the inhibitor. Such dependence of locomotion on chemical and diffusive mechanisms might be used by cells as mechanisms to control their behavior. By exploiting the inertial motion, an amoebic cell would avoid from being trapped into local maxima of concentration or it might turn around on its enemies or foods to catch them. It remains for a future work to elucidate whether the inertial motion is advantageous to cells in their physiological conditions.

This work was supported by the ACT-JST project of the Japan Science and Technology Corporation and by a Grant-in-Aid for the 21st Century COE for Frontiers of Computational Science.

[1] C. A. Parent, Curr. Opin. Cell Biol. **16**, 4 (2004).
[2] M. Iijima, Y. E. Huang, and P. Devreotes, Dev. Cell **3**, 469 (2002).
[3] V. L. Katanaev, Biochemistry (Mosc.) **66**, 351 (2001).
[4] P. C. Wilkinson, J. Immunol. Methods **216**, 139 (1998).
[5] A. Levchenko and P. A. Iglesias, Biophys. J. **82**, 50 (2002).
[6] M. Ueda, Y. Sako, T. Tanaka, P. Devreotes, and T. Yanagida, Science **5543**, 864 (2001).
[7] N. Li Jeon, H. Baskaran, S. K. W. Dertinger, G. M. Whitesides, L. V. D. Water, and M. Toner, Nat. Biotechnol. **20**, 826 (2002).
[8] A. B. Verkhovsky, T. M. Svitkina, and G. G. Borisy, Curr. Biol. **9**, 11 (1999).
[9] T. D. Pollard and G. G. Borisy, Cell **112**, 453 (2003).
[10] A. F. M. Marée and P. Hogeweg, Proc. Natl. Acad. Sci. U.S.A. **98**, 3879 (2001).
[11] J. A. Izaguirre, R. Chaturvedi, C. Huang, T. Cickovski, J. Coffland, G. Thomas, G. Forgacs, M. Alber, G. Hentschel, S. A. Newman, and J. A. Glazer, Bioinformatics **20**, 1129 (2004).